ChemComm

COMMUNICATION

View Article Online
View Journal | View Issue

Cite this: *Chem. Commun.*, 2025, **61**, 16274

Received 7th July 2025,
Accepted 2nd September 2025

DOI: 10.1039/d5cc03810c

rsc.li/chemcomm

Alkyl-chain-grafted 13X zeolite for steady CO_2 capture from humid flue gas

Beining Cao,[ab] Qian Jia,[*a] Guoqiang Li,[a] Haitao Cui,[a] Feng Li,[a] Bo Peng*[c] and Lei Li*[a]

13X zeolite shows potential for CO_2 capture, but its performance is diminished by the steam present in real-world flue gas. To overcome this limitation, a facile and efficient approach is to graft straight-chain alkyl groups to the 13X structure. Adsorbents with anchored alkyl groups exhibit both high CO_2 uptake and excellent resistance to humidity.

Anthropogenic CO_2 emissions pose a significant threat to global climate stability.[1] To address this issue, the following technical routes have been proposed: (1) direct air capture (DAC),[2] which extracts CO_2 directly from the atmosphere (420 ppm CO_2); and (2) point-source carbon capture,[3] primarily applied in industrial sectors with high-concentration CO_2 emissions. Nowadays, industrial sectors, such as power plants and petrochemical industries, contribute to over 25% of global carbon emissions.[4] Therefore, it is essential to develop high-performance adsorbents for CO_2 removal from flue gas. However, efficient CO_2 capture remains challenging, mainly due to the negative impact of the water vapor in flue gas (~10 vol%) on CO_2 adsorption.[5] Physical adsorption generally describes the adherence of an adsorbate to the surface of an adsorbent through weak interactions, such as van der Waals forces and electrostatic forces, without involving the making or breaking of chemical bonds, and typically occurs in a reversible fashion. Physical adsorbents typically exhibit stronger affinity for H_2O, due to its dipole moment, compared to CO_2, which relies on weaker quadrupolar interactions.[6] Thus, water vapor competitively adsorbs with CO_2, reducing overall CO_2 uptake. For example, at 90% relative humidity (3.4 vol%), the CO_2 capture capacity of 13X zeolite is reduced by 18.5% after multiple vacuum swing adsorption cycles.[7] Similarly, the static CO_2 adsorption capacity of Na-LSX zeolite was reduced by 50% following exposure to moisture pretreatment conditions.[8]

To mitigate the impact of humidity, pure silica materials[9] and carbon materials with a hydrophobic nature[10,11] were previously used as CO_2 adsorbents because of their low affinity for H_2O molecules. However, this improved resistance to humidity was normally achieved by sacrificing CO_2/N_2 selectivity. Zeolites, 3-dimensional crystalline structures constructed from SiO_4^{4-} tetrahedra bridged by O atoms, offer an alternative. Although substituting Si atoms with elements like Al generates an overall negatively charged framework that attracts neutralizing cations (*e.g.*, H^+, Na^+, Ca^{2+}, and La^{3+}) and enhances hydrophilicity, zeolites remain highly promising for CO_2 capture, as these incorporated cations can promote strong interactions with CO_2 and lead to high CO_2/N_2 selectivity.[11,12]

To prohibit water vapor access, several feasible strategies have been proposed to modify zeolite surfaces: (1) polymerizing polyethylene terephthalate (PET) films on the zeolite surface,[13] (2) combining ZIF materials with zeolites *via* a glass transition,[14] (3) utilizing azide reagents as binders for composites,[15] *etc.* However, these methods are complicated and may not be suitable for large-scale applications.

In this work, an efficient approach was introduced by grafting different alkyl molecules onto 13X zeolite *via* methanol condensation between hydroxyl groups of zeolite and methoxy groups of silanes (Fig. 1a and b).[16] Alkyl chains with different carbon numbers were tested, *i.e.* trimethoxy(propyl)silane (3C), hexyltrimethoxysilane (6C), and dodecyltrimethoxysilane (12C). It is important to note that the kinetic diameter of hexyltrimethoxysilane (~1.1 nm) fits the largest pore opening of 13X zeolite. The influence of alkyl-modified zeolites on the CO_2 adsorption performance has been investigated under humid flue gas conditions. The modified pore structure endows the material with remarkable CO_2 adsorption capacity, water resistance and excellent cycling stability, suggesting potential applications for post-combustion CO_2 capture.

According to the sol–gel poisoned Eden model, the three methoxy groups from the grafting agent can undergo two

[a] *State Key Laboratory of Coal Conversion, Institute of Coal Chemistry, Chinese Academy of Sciences, Taiyuan, 030001, P. R. China. E-mail: lilei@sxicc.ac.cn*
[b] *University of the Chinese Academy of Sciences, Beijing, 100049, P. R. China*
[c] *SINOPEC Research Institute of Petroleum Processing Co., Ltd., Beijing 100083, P. R. China*

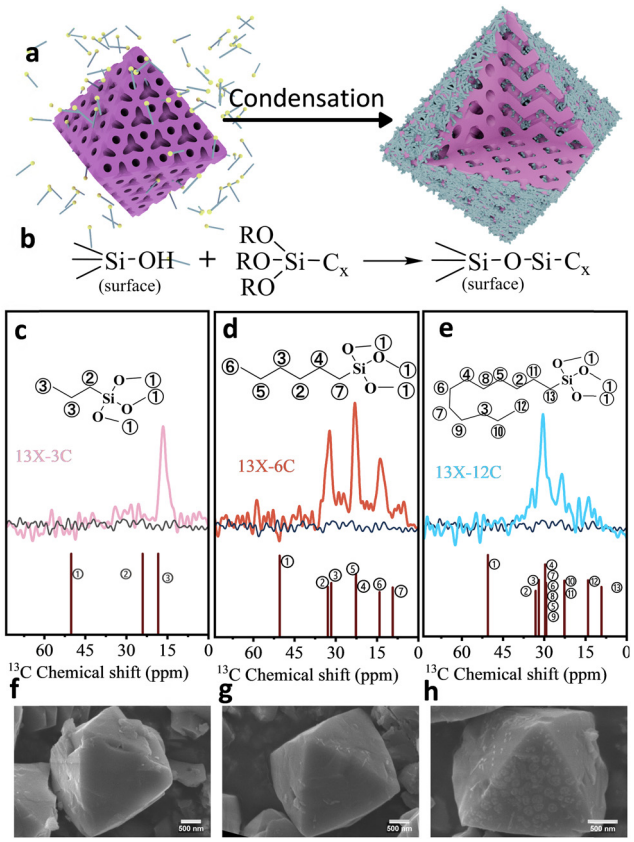

Fig. 1 (a) A schematic diagram of the formation of alkyl-chain-grafted zeolite. (b) The condensation reaction of silanol with methoxy groups. Solid-state ^{13}C NMR spectra of 13X-3C and trimethoxy(propyl)silane (c), 13X-6C and hexyltrimethoxysilane (d), and 13X-12C and dodecyltrimethoxysilane (e). SEM images of 13X-3C (f), 13X-6C (g), and 13X-12C (h).

competing reactions: (1) condensation with surface hydroxy groups of zeolite or (2) self-condensation to form a low-fractal dimension[16] and loosely structured carbon layer. The presence of hydroxyl groups in the zeolite can be confirmed by the broad Fourier transform infrared spectroscopy absorption peaks within the range of 3500–3100 cm^{-1} and ^{1}H NMR peaks at 1.2 ppm (silanol groups) and 3.6 ppm (bridging oxygen hydroxyl groups) (Fig. S5 and S13). Compared with the ^{13}C NMR spectra of the pure grafting agents (Fig. 1c–e), the disappearance of the methoxy signal (50 ppm; ①) from modified zeolite indicated condensation between the methoxy and surface hydroxyl groups. In addition, the attenuated signals at 9.3 ppm (⑦ and ⑬) for 13X-6C and 13X-12C after grafting suggest a significant change in the local chemical environment for carbons adjacent to silicon atoms. To see the effect of the grafted groups, the crystalline structures of modified zeolites were compared with their parent materials (Fig. S2), and this shows that the introduction of alkyl molecules has no effect on the crystallinity, but the diffraction peaks shift slightly towards higher angles, which has a certain impact on the periodicity of the material.

SEM confirmed that the grafting of alkyl molecules can form a carbon layer on the zeolite surface (Fig. 1f–h). In addition,

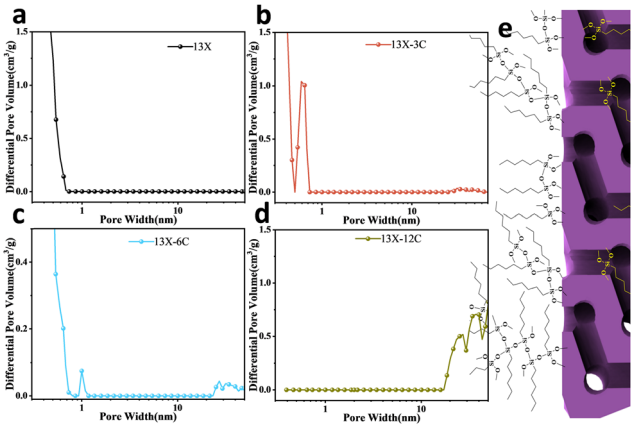

Fig. 2 The aperture distributions of (a) 13X, (b) 13X-3C, (c) 13X-6C, and (d) 13X-12C, and (e) a schematic diagram of the structure of modified 13X.

prominent interparticle adhesion of carbon layers can be detected on 13X-12C, which is a consequence of the dispersion of longer chain molecules combined with silane condensation among methoxy groups (Fig. S3h). N_2 adsorption isotherms (at 77 K) exhibited a slight reduction in pore volume for modified zeolites, possibly due to the relatively small mass contribution of the alkyl groups (Fig. S6). The NLDFT model was applied to analyze the pore size distribution within the structure.[17] Notably, both 13X-3C and 13X-6C displayed additional apertures of around 1 nm and 30 nm (Fig. 2). The presence of these apertures can be tentatively attributed to the entanglement of alkyl groups fixed on the zeolite surface. Depending on the locations of alkyl groups, the small aperture (13X-3C: 0.6 nm) was probably created within the zeolite pores, while the large aperture (30 nm) was formed by grafted alkyl molecules on the outer surface. In contrast, 13X-dodecyl only exhibited the large aperture (30–40 nm). This can be explained by the reduced pore aperture with long-chain alkyl groups, which cause severe pore blockages and hinder nitrogen diffusion in the low-pressure range. Thus, its micropore characteristics are masked by mesoporous pores.

The relevant contact angle measurements also verified the modification of the material surface with alkyl groups (Fig. S4). Upon increasing the length of alkyl chains, the resistance of the carbon layer to water molecules was more pronounced, as indicated by the higher contact angle for the zeolites 13X-hexyl (158.2°) and 13X-dodecyl (145.5°). The thermal decomposition behaviour of the modified alkyl groups was characterized using DSC (Fig. 3a). The peaks at 360 °C and 416 °C were assigned to the loss of alkyl groups. Due to the Brønsted acidity of zeolite[18] and the confinement effect on alkyl groups,[19] the thermal decomposition temperature of the modified alkyl groups in the zeolite phase is lower than that of the alkyl groups themselves. Therefore, the peak at 360 °C originated from the modified alkyl groups in the zeolite phase,[19] while the peak at 416 °C was related to the outer carbon layer structure on the zeolite surface originating from the self-condensation of the grafted silanes. For small-sized groups, such as propyl, the exothermic peak (360 °C) indicates that the modified alkyl

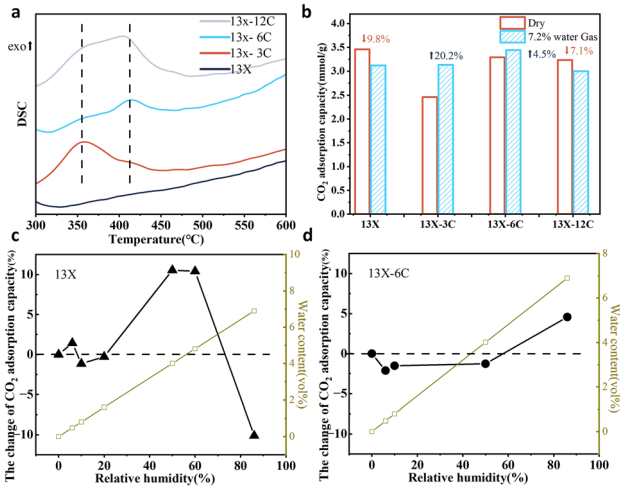

Fig. 3 (a) DSC curves of modified zeolites under an oxygen atmosphere compared to pristine 13X. (b) A comparison between CO_2 uptake under dry and humid conditions at 41 °C; the water vapor content is 7.2%. The variation in the CO_2 adsorption capacity of 13X (c) and 13X-6C (d) at different levels of relative humidity (RH) compared to dry conditions.

groups are largely present in the zeolite phase, while 13X-6C and 13X-12C maintain a relatively high exothermic peak at 416 °C, indicating the presence of abundant silane-based carbon layer structures on the zeolite surface.

The performance of zeolite adsorbents was assessed by measuring CO_2 adsorption in a fixed-bed reactor (Fig. S1). Fig. 3b shows the CO_2 uptake from dynamic column breakthrough experiments at 41 °C using standard feed gas simulating real-world flue gas (7.2% H_2O, 13.92% CO_2 and 78.88% N_2 vs 15% CO_2 and 85% N_2). Under dry conditions, the CO_2 uptake of 13X-3C was reduced compared to its counterparts. This can be attributed to the higher content of alkyl groups in the zeolite pores. As such, CO_2 transport will be affected, resulting in lower uptake. In contrast, the bulkier hexyl and dodecyl groups were partially or even largely fixed on the outer surface, resulting in a slight change in CO_2 uptake. However, under humid conditions, the adsorbent with dodecyl groups displayed a significant drop in CO_2 uptake, similar to 13X. In contrast, the CO_2 uptake of 13X-3C and 13X-6C increased, suggesting the enhancing effect of water vapor on CO_2 uptake in the presence of such alkyl groups in the pore structure. This could be related to the improved water resistance of zeolites, by which the adsorbed amount of water vapor was reduced. In general, the smaller propyl and hexyl groups have a more pronounced effect on the water resistance of zeolite adsorbents compared to dodecyl groups, but propyl molecules can easily access the pore structure, hindering CO_2 diffusion. In this context, 13X-6C was optimum for application in flue gas treatment due to its stable CO_2 adsorption performance under both dry and humid conditions. Therefore, only 13X-6C is discussed in terms of further investigations.

The influence of water vapor on CO_2 adsorption was studied. Fig. 3c and d compares the CO_2 adsorption capacities of zeolite adsorbents at varying relative humidity levels. Different scenarios are shown for the original 13X and modified 13X-6C adsorbents. At lower humidity (<20%), the presence of water had a negligible effect on the CO_2 uptake by both materials. However, at a higher water content, an increase in CO_2 uptake was detected for 13X, which could be related to the formation of carbonates according to previous studies,[20,21] while the CO_2 adsorption of 13X-6C remained nearly constant. When the relative humidity exceeded 80%, the CO_2 uptake from 13X experienced a dramatic drop, whereas 13X-6C showcased an appreciable increase in CO_2 uptake. A possible explanation is that water molecules easily cluster into the pore structure of unmodified 13X, reducing the available space. However, the inclusion of alkyl groups hindered the transport of water molecules and prohibited the formation of water clusters.[22,23] Water vapor adsorption was measured (Fig. S12), and this indicated that grafting alkyl groups can reduce the saturated adsorption capacity of H_2O. In addition, the heat of H_2O adsorption from 13X and 13X-6C was estimated using two-cycle DSC measurements by integrating the desolvation peak (Fig. S10). Compared with 13X, the heat of water vapor adsorption for 13X-6C shows a slight decrease, but its desorption temperature does not change significantly, indicating that the alkyl groups do not alter the adsorption characteristics of the zeolite towards water.

To further explore the influence of alkyl groups on the water vapor adsorption dynamics, the mutual diffusion and self-diffusion of H_2O molecules were studied. For mutual diffusion, the radial diffusion model[24] is used to determine the initial-stage diffusion coefficient (D) of H_2O molecules, and the intraparticle diffusion model[25] is employed to measure the adsorption rate constant of H_2O molecules (k_w) in the final stage of adsorption. At low water vapor pressure (50.7 Pa, Fig. 4a), D values for 13X-6C are significantly smaller than those for pristine 13X, indicating that hexyl grafting effectively inhibits the diffusion of H_2O molecules in the initial stage (Fig. 4a); and in the final stages, the smaller differences in the k_w values of the two suggest a reduced variation in the adsorption rate. At low vapor pressure, two models are required to represent the diffusion patterns in different time periods, indicating a change in the diffusion mechanism: the dominant diffusion mode seems to shift from molecular diffusion at low vapor loading to intracrystalline diffusion at higher vapor loading (Fig. 4a).[26] However, the alkyl-group inhibition effect becomes less pronounced at elevated vapor loadings (approximately 82.3%, Fig. 4b), where the diffusion coefficients for both initial and final stages converge. This convergence indicates that alkyl modification primarily influences H_2O molecule diffusion under low-loading conditions, while its impact diminishes appreciably when approaching saturation.

For the self-diffusion of molecules, the adsorption and equilibrium diffusion of water vapor on 13X and 13X-6C were simulated using grand canonical Monte Carlo (GCMC) and molecular dynamics (MD) methods.[27] The randomly selected diffusion paths of water molecules in the MD simulations are shown in Fig. S14. The probability of H_2O molecules passing through the zeolite cavity after alkyl modification decreased. Moreover, the self-diffusion coefficient of water molecules

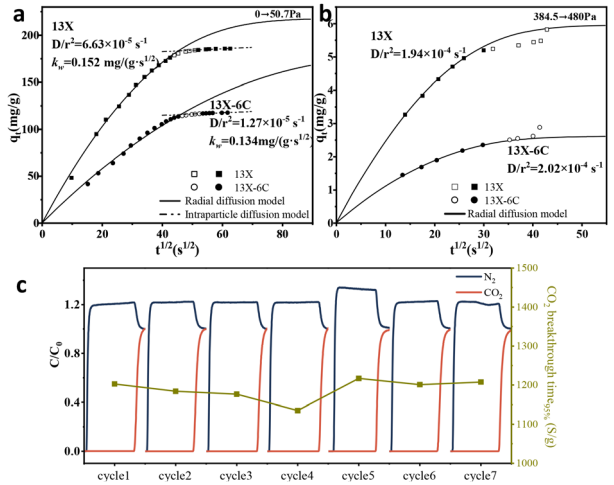

Fig. 4 The relationship between time and water vapor adsorption capacity for 13X and 13X-6C at 50.9 Pa (a) and 480 Pa (b) (solid lines: theoretical values using the radial diffusion model, dashed lines: theoretical values using the intraparticle diffusion model, black squares: experimental data from 13X, black circles: experimental data from 13X-6C); the saturated vapor pressure at 41 °C is 7778 Pa. (c) The CO_2 breakthrough curves of 13X-6C tested using simulated flue gas feed (7.2 wt% H_2O) over seven cycles.

decreased for alkyl-modified zeolites (Table S1). Finally, the cycling stability of modified 13X-6C was evaluated (Fig. 4c). During the measurements, the same batch of 13X-6C was tested 7 times using $CO_2/N_2/H_2O$ mixed gas (13.89/78.88/7.2 v/v/v). Its adsorption capacity remained at around 3.46 mmol g^{-1}, and the performance did not decline.

In conclusion, hydrophobic alkyl molecules can anchor either within pores or on the surface of zeolites, depending on their molecular size. This differential anchoring manner creates micropores (for smaller molecules) or mesopores (for larger ones). The resulting alkyl-modified zeolite shows improved water vapor resistance, which is favourable for post-combustion CO_2 capture. Breakthrough experiments under simulated flue gas conditions indicate that the CO_2 adsorption capacity of 13X zeolite shows the phenomenon of first increasing and then decreasing with an increase in humidity. Moreover, zeolite with appropriate alkyl modification has lower sensitivity to humidity changes. Furthermore, through a study of water diffusion, it was found that alkyl inhibition of water diffusion occurs when the water loading is low, which is a key point. This provides a new perspective relating to the bed layer diffusion kinetics of the actual adsorption process.

The project was supported by the National Natural Science Foundation of China (U23A20100), Key R&D Program of Shanxi Province (202202090301013, 202102090301008), ICC CAS SCJC-DT-2023-03, and the independent research project of the State Key Laboratory of Coal Conversion (2024BWZ006)

Conflicts of interest

There are no conflicts to declare.

Data availability

The data supporting this article are included in the SI. See DOI: https://doi.org/10.1039/d5cc03810c.

Notes and references

1 S. Solomon, G.-K. Plattner, R. Knutti and P. Friedlingstein, *Proc. Natl. Acad. Sci. U. S. A.*, 2009, **106**, 1704–1709.
2 A. Goeppert, M. Czaun, G. K. Surya Prakash and G. A. Olah, *Energy Environ. Sci.*, 2012, **5**, 7833–7853.
3 A. G. Olabi, T. Wilberforce, K. Elsaid, E. T. Sayed, H. M. Maghrabie and M. A. Abdelkareem, *J. Cleaner Prod.*, 2022, **362**, 132300.
4 B. Metz, O. Davidson, H. De Coninck, M. Loos and L. Meyer, *IPCC special report on carbon dioxide capture and storage*, Cambridge University Press, Cambridge, 2005.
5 R. Zevenhoven and P. Kilpinen, *Control of pollutants in flue gases and fuel gases*, Helsinki University of Technology, Espoo, Finland, 2001.
6 N. Hedin, L. Chen and A. Laaksonen, *Nanoscale*, 2010, **2**, 1819–1841.
7 G. Li, P. Xiao, P. Webley, J. Zhang, R. Singh and M. Marshall, *Adsorption*, 2008, **14**, 415–422.
8 F. Brandani and D. M. Ruthven, *Ind. Eng. Chem. Res.*, 2004, **43**, 8339–8344.
9 L. Ronchi, H. Nouali, T. J. Daou, J. Patarin and A. Ryzhikov, *New J. Chem.*, 2017, **41**, 15087–15093.
10 D. Xu, P. Xiao, J. Zhang, G. Li, G. Xiao, P. A. Webley and Y. Zhai, *Chem. Eng. J.*, 2013, **230**, 64–72.
11 S. De, A. M. Balu, J. C. van der Waal and R. Luque, *ChemCatChem*, 2015, **7**, 1608–1629.
12 D. Bonenfant, M. Kharoune, P. Niquette, M. Mimeault and R. Hausler, *Sci. Technol. Adv. Mater.*, 2008, **9**, 013007.
13 A. Zhou, C. Yang, M. Xue, B. Xue, J. Zheng, X. Li, F. Nie, X. Zhao and J. Mi, *Sep. Purif. Technol.*, 2025, **355**, 129689.
14 S. Chi, Y. Ye, X. Zhao, J. Liu, J. Jin, L. Du and J. Mi, *Sep. Purif. Technol.*, 2023, **307**, 122738.
15 D.-i Kwon, J.-C. Kim, H. Lee, W. Lee and C. Jo, *Chem. Eng. J.*, 2022, **427**, 131461.
16 C. J. Brinker and G. W. Scherer, *Sol-gel science: the physics and chemistry of sol-gel processing*, Academic press, 2013.
17 C. Lastoskie, K. E. Gubbins and N. Quirke, *J. Phys. Chem.*, 1993, **97**, 4786–4796.
18 P. del Campo, C. Martínez and A. Corma, *Chem. Soc. Rev.*, 2021, **50**, 8511–8595.
19 W. Wang, J. Jiao, Y. Jiang, S. S. Ray and M. Hunger, *Chem. Phys. Chem.*, 2005, **6**, 1467–1469.
20 R. V. Siriwardane, M.-S. Shen and E. P. Fisher, *Energy Fuels*, 2003, **17**, 571–576.
21 H. Veldhuizen, S. A. Butt, A. van Leuken, B. van der Linden, W. Rook, S. van der Zwaag and M. A. van der Veen, *ACS Appl. Mater. Interfaces*, 2023, **15**, 29186–29194.
22 B. S. Bal'zhinimaev, E. A. Paukshtis, A. V. Toktarev, E. V. Kovalyov, M. A. Yaranova, A. E. Smirnov and S. Stompel, *Microporous Mesoporous Mater.*, 2019, **277**, 70–77.
23 J. Hunger, I. A. Beta, H. Böhlig, C. Ling, H. Jobic and B. Hunger, *J. Phys. Chem. B*, 2006, **110**, 342–353.
24 J. Crank, *The mathematics of diffusion*, Oxford University Press, 1979.
25 F.-C. Wu, R.-L. Tseng and R.-S. Juang, *Chem. Eng. J.*, 2009, **153**, 1–8.
26 D. M. Ruthven, *Principles of adsorption and adsorption processes*, John Wiley & Sons, 1984.
27 D. Dubbeldam, S. Calero, D. E. Ellis and R. Q. Snurr, *Mol. Simul.*, 2016, **42**, 81–101.